Technical Report

TR-2015-011

HIGAMod: A Hierarchical IsoGeometric Approach for MODel reduction in curved pipes

by

S. Perotto, A. Reali, P. Rusconi, A. Veneziani

Mathematics and Computer Science

EMORY UNIVERSITY

HIGAMod: A Hierarchical IsoGeometric Approach for MODel reduction in curved pipes

S. Perotto[♯], A. Reali[†‡], P. Rusconi[♭], A. Veneziani[♮]

November 3, 2015

[♯] MOX, Dipartimento di Matematica, Politecnico di Milano
Piazza Leonardo da Vinci 32, 20133 Milano, Italy
[†] Department of Civil Engineering and Architecture, University of Pavia
via Ferrata 3, 27100, Pavia, Italy
[‡] Institute for Advanced Study, Technische Universität München
Lichtenbergstraße 2a, 85748 Garching, Germany
[♭] Politecnico di Milano, Piazza Leonardo da Vinci 32, 20133 Milano, Italy
[♮] Department of Mathematics and Computer Science, Emory University
400 Dowman Dr., Atlanta, GA 30322, USA
simona.perotto@polimi.it; alessandro.reali@unipv.it;
paolo2.rusconi@mail.polimi.it; ale@mathcs.emory.edu

Keywords: Hierarchical Model Reduction, IsoGeometric Analysis, Fluid Dynamics in Curved Pipes

AMS Subject Classification: 65N30, 76M10, 76M22

Abstract

In computational hemodynamics we typically need to solve incompressible fluids in domains given by curved pipes or network of pipes. To reduce the computational costs, or conversely to improve models based on a pure 1D (axial) modeling, an approach called "Hierarchical Model reduction" (HiMod) was recently proposed. It consists of a diverse numerical approximation of the axial and of the transverse components of the dynamics. The latter are properly approximated by spectral methods with a few degrees of freedom, while classical finite elements were used for the main dynamics to easily fit any morphology. However affine elements for curved geometries are generally inaccurate. In this paper we conduct a preliminary exploration of IsoGeometric Analysis (IGA) applied to the axial discretization. With this approach, the centerline is approximated by Non Uniform Rational B-Splines (NURBS). The same functions are used to represent the axial component of the solution. In this way we obtain an accurate representation of the centerline as well as an accurate representation of the

solution with few axial degrees of freedom. This paper provides preliminary promising results of the combination of HiMod with IGA - referred to as HIGAMod approach - to be applied in any field involving computational fluid dynamics in generic pipe-like domains.

1 Introduction

Progressive application of computational mechanics to real life problems challenges both hardware architectures and numerical methodologies to fit the timelines requested by the applications. As a reference application, we mention computational hemodynamics in arteries of real patients to support medical research and most importantly clinical practice [17]. In order to accelerate the numerical simulation of incompressible fluids, we can customize standard methods to take advantage of particular features of the problem to solve, like the shape of the region of interest and the consequent peculiarities of the fluid dynamics. Specifically, for pipe-like domains like arteries we proposed a combination of finite elements and spectral methods, following the natural decomposition of a mainstream dynamics (solved with FEM) and the transverse components (solved with a modal approximation) [16, 29]. As the transverse components are expected to have a minor impact on the global dynamics, a few spectral degrees of freedom (DOF) are usually enough, resulting in smaller discrete problems to solve with respect to standard methods, with an evident computational advantage. We called this approach Hierarchical Model Reduction (HiMod) since it yields a "psychologically 1D" approximation where the accuracy for transverse dynamics can be hierarchically tuned by a proper (even automatic) selection of the number of spectral DOF. The method merges the versatility of finite elements and the accuracy of spectral approximations to attain a reduction of computational costs - an introduction can be found in [27]. We recall the basic properties in Sect. 2.

One of the limitations of this method - in its original form - relies on the rectilinear nature of the centerline defining the axis of the pipe. As a matter of fact, for curved pipes the method can be applied by rectifying the centerline with a piecewise affine map. In a more sophisticated setting, we may consider classical (one dimensional) isoparametric finite elements. Although these strategies are viable and work as expected [28], in the search of more sophisticated and performing methods, in this paper we propose to use isogeometric elements as an alternative for the mainstream dynamics on curved pipes. IsoGeometric Analysis (IGA) is a relatively recent idea proposed by T.J.R. Hughes and coworkers [21] that replaces piecewise polynomial functions of the standard FEM with Non Uniform Rational B-Splines (NURBS) popular in Computer Aided Design applications - often used for the preliminary processing of the geometry of interest for a simulation. There are many advantages of this approach in practice, ranging from the contiguity of the treatment of the geometry of interest and the solution of the problem solved there, to the accuracy obtained with

relatively few degrees of freedom. We recall basic properties of IGA in Sect. 3.1.

In this respect, the pairing of HiMod and IGA (called hereafter HIGAMod) seems a natural approach for the acceleration of fluid dynamics solution in curved pipes. This paper intends to introduce this idea (Sect. 3.2) and to provide preliminary results corroborating the expectations. In fact, on tests covering both academic test cases with an analytical solution and nontrivial geometries - reported in Sect. 4 - the effectiveness of HIGAMod is confirmed in comparison with standard finite element approaches. This is the first work on HIGAMod, that motivates its extension to more realistic, challenging - and hopefully performing - applications.

2 The HiMod setting

Let us introduce the geometrical prerequisites we postulate for the HiMod formulation of a generic differential problem in the weak form

$$\text{find } u \in V \ : \ a(u,v) = F(v) \quad \forall v \in V, \tag{1}$$

where V is a Hilbert space with norm $\|\cdot\|_V$, $a(\cdot,\cdot) : V \times V \to \mathbb{R}$ and $F(\cdot) : V \to \mathbb{R}$ are a bilinear and a linear form, respectively. We assume (1) to be well posed after suitable hypotheses. The independent variables are assumed to belong to the domain $\Omega \subset \mathbb{R}^d$ $(d = 2, 3)$ that we conceptualize as a fiber bundle, where we distinguish a supporting one-dimensional curved domain Ω_{1D} aligned with the centerline (corresponding to the mainstream dynamics), and a set of $(d-1)$-dimensional sections or fibers $\gamma \subset \mathbb{R}^{d-1}$ orthogonal to the centerline and associated with the transverse secondary dynamics. We denote by $\Psi : \Omega \to \widehat{\Omega}$ the map between the physical domain Ω and a reference domain $\widehat{\Omega} = \widehat{\Omega}_{1D} \times \widehat{\gamma}_{d-1}$, where $\widehat{\Omega}_{1D}$ is a rectilinear fiber and $\widehat{\gamma}_{d-1}$ is the reference $(d-1)$ dimensional transverse reference fiber. More precisely, we denote by $\mathbf{z} = (x, \mathbf{y})$ and by $\widehat{\mathbf{z}} = (\widehat{x}, \widehat{\mathbf{y}})$ a generic point in Ω and the corresponding point in $\widehat{\Omega}$, respectively such that $\widehat{\mathbf{z}} = \Psi(\mathbf{z}) = (\Psi_1(\mathbf{z}), \Psi_2(\mathbf{z}))$, with $\widehat{x} = \Psi_1(\mathbf{z})$ and $\widehat{\mathbf{y}} = \Psi_2(\mathbf{z})$. As Ω_{1D} coincides with the centerline of the domain Ω, likewise $\widehat{\Omega}_{1D}$ is the centerline of the reference domain. The inverse map to Ψ, $\Phi : \widehat{\Omega} \to \Omega$, is defined by $\mathbf{z} = \Phi(\widehat{\mathbf{z}}) = (\Phi_1(\widehat{\mathbf{z}}), \Phi_2(\widehat{\mathbf{z}}))$, with $x = \Phi_1(\widehat{\mathbf{z}})$ and $\mathbf{y} = \Phi_2(\widehat{\mathbf{z}})$. We assume both the maps Ψ and Φ to be differentiable with respect to $\mathbf{z}$ and $\widehat{\mathbf{z}}$ respectively. The splitting in main and transverse components - and consequently the maps Ψ and Φ - play a crucial role in the HiMod construction. In this respect, let $V_{\widehat{\Omega}_{1D}}$ be a one-dimensional space of functions compatible with the boundary conditions assigned along the extremal faces of Ω. We introduce the finite dimensional space

$$V_m = \left\{ v_m(\mathbf{z}) = \sum_{k=1}^{m} v_k(\Psi_1(\mathbf{z}))\varphi_k(\Psi_2(\mathbf{z})), \text{ with } v_k \in V_{\widehat{\Omega}_{1D}} \right\}$$

for a given modal index $m \in \mathbb{N}^+$, where $\{\varphi_k\}_{k \in \mathbb{N}^+}$ represents a modal basis of functions orthonormal with respect to the L^2-scalar product on $\widehat{\gamma}_{d-1}$ and

taking into account the boundary conditions imposed on the lateral surfaces of Ω. Space V_m states a hierarchy of reduced models marked by the modal index m, where all the functions involved are defined on the reference domain via the map Ψ. To guarantee the well-posedness and the convergence to u of the HiMod approximation $u_m \in V_m$ such that

$$a(u_m, v_m) = F(v_m) \quad \forall v_m \in V_m, \tag{2}$$

we postulate *conformity* of V_m ($V_m \subset V, \forall m \in \mathbb{N}^+$) as well as *spectral approximability* ($\lim_{m\to+\infty}(\inf_{v_m\in V_m} \|v - v_m\|_V) = 0, \forall v \in V$).

Through the HiMod reduction we rewrite (2) as a system of m coupled 1D problems. This implies a significant reduction of the number of degrees of freedom with respect to a traditional finite element discretization (in particular in 3D) whenever transverse dynamics can be captured by a relatively low number m of modes - as it is often the case in real applications. To this aim, let us set in (2) $u_m(\mathbf{z}) = \sum_{j=1}^m u_j(\Psi_1(\mathbf{z}))\varphi_j(\Psi_2(\mathbf{z}))$ and identify v_m with the product $\vartheta(\Psi_1(\mathbf{z}))\varphi_k(\Psi_2(\mathbf{z}))$, where ϑ and u_j, $j = 1, \ldots, m$, belong to $V_{\widehat{\Omega}_{1D}}$. Here, the modal coefficients u_j are the unknowns. For the sake of exemplification, let us assume that (1) refers to linear advection diffusion reaction (ADR) problem,

$$-\mu\Delta u + \mathbf{b}\cdot\nabla u + \sigma u = f \quad \text{in } \Omega, \tag{3}$$

where f is the source term corresponding to the linear form F in (1), $\mu, \mathbf{b}$ and σ are given coefficients, completed by homogeneous Dirichlet conditions on the boundary Γ_D, Neumann conditions on Γ_N, Robin conditions on Γ_R so that $\partial\Omega = \Gamma_D \cup \Gamma_N \cup \Gamma_R$ and each portion of the boundary has null measure intersection with the others. In fact, in the last section of the present work we will consider this problem as well as more complicated ones, like the Stokes equations for incompressible fluids. In particular, the lateral surfaces of the pipe will be assumed to be part of Γ_D, the extension of HiMod to more general cases being considered in [3]. The discretized HiMod problem then reads: find $u_j \in V_{\widehat{\Omega}_{1D}}$ with $j = 1, \ldots, m$, such that, for any $\vartheta \in V_{\widehat{\Omega}_{1D}}$ and $k = 1, \ldots, m$,

$$\begin{aligned}
&\sum_{j=1}^{m} \Bigg\{ \int_{\widehat{\Omega}_{1D}} \Big[\widehat{r}_{kj}^{\,1,1}(\widehat{x})\, u_j'(\widehat{x})\, \vartheta'(\widehat{x}) \,+\, \widehat{r}_{kj}^{\,1,0}(\widehat{x})\, u_j'(\widehat{x})\, \vartheta(\widehat{x}) \\
&\qquad + \widehat{r}_{kj}^{\,0,1}(\widehat{x})\, u_j(\widehat{x})\, \vartheta'(\widehat{x}) + \widehat{r}_{kj}^{\,0,0}(\widehat{x})\, u_j(\widehat{x})\, \vartheta(\widehat{x}) \Big]\, d\widehat{x} \Bigg\} \\
&= \int_{\widehat{\Omega}_{1D}} \Big[\int_{\widehat{\gamma}_{d-1}} f(\Phi(\widehat{\mathbf{z}}))\varphi_k(\widehat{\mathbf{y}}) |\mathcal{J}^{-1}(\Phi(\widehat{\mathbf{z}}))|\, d\widehat{\mathbf{y}} \Big] \vartheta(\widehat{x})\, d\widehat{x},
\end{aligned} \tag{4}$$

$\mathcal{J} = \partial\Psi/\partial\mathbf{z} \in \mathbb{R}^{d\times d}$ denotes the Jacobian associated with the map Ψ. The HiMod coefficients $\widehat{r}_{kj}^{\,s,t}$, with $s, t = 0, 1$ and $k, j = 1, \ldots, m$, are computed on the reference fiber via map Ψ, as

$$\widehat{r}_{kj}^{\,s,t}(\widehat{x}) = \int_{\widehat{\gamma}_{d-1}} r_{kj}^{s,t}(\widehat{x}, \widehat{\mathbf{y}})\, |\mathcal{J}^{-1}(\Phi(\widehat{\mathbf{z}}))|\, d\widehat{\mathbf{y}},$$

whereas the full coefficients $r_{kj}^{s,t}$ involve the problem data, the modal functions φ_j and φ_k, and the components $\partial\Psi_i/\partial x$, $\nabla_{\mathbf{y}}\Psi_i$ $(i = 1, 2)$ of the Jacobian $\mathcal{J}$, with $\nabla_{\mathbf{y}}$ the gradient with respect to $\mathbf{y}$. An explicit computation of these coefficients can be found in [16] for a rectilinear Ω_{1D} and in [28] for a generically curved fiber Ω_{1D}. As expected, the latter case is much more complicated. It may be worth noting that the HiMod reduced problem does not necessarily reflects the nature of the full problem, for instance a purely diffusive full problem reduces to a set of "psychologically 1D" advection-reaction problems (see [29, 3] for the details).

For particular choices of the discretization methods and of the storing of the algebraic coefficients, the system we obtain features a pattern that reflects blockwise the 1D discretization along the axis, with clear computational advantages in the linear algebra. In addition, a judicious selection of m can introduce several computational improvements (see [27] for a survey). As a matter of fact, the basic method considers a *uniform* constant selection of m along Ω_{1D}; however, different values may be considered in different subdomains of Ω (*piecewise* HiMod reduction [30]); alternatively, each degree of freedom of the axial problem can be associated with a different number of modes as done in [31, 32] (*pointwise* HiMod reduction). In any case, the specific number of modes can be selected *a priori*, driven by a partial physical knowledge of the phenomenon at hand [16, 29], or automatically via an adaptive model reduction procedure based on an *a posteriori* modeling error analysis [30, 32]. This adaptivity conveniently combines with mesh adaptive procedures along the centerline.

As pointed out above, the rationale of the HiMod formulation relies on using different discretization techniques for the two directions. Originally, we considered the axial components approximated by classical finite elements while the transverse ones on γ_{d-1} by a spectral approximation. This choice was motivated by the simplicity of 1D finite elements as well as by their versatility in representing pipes with a generic centerline. From a different standpoint, we can regard HiMod as a way for improving 1D network models of the circulatory system [9, 17] (as well as oil pipelines, internal combustion engines, river systems, etc.) with a local enhancement introduced by low cost spectrally approximated transverse components [2, 10]. In particular in [28] a piecewise linearization of a curved pipe was explored. While this guarantees easiness of implementation, piecewise affine approximation of the curved centerline may introduce some accuracy degradation and using fine meshes along the axis to balance this does not seem the best approach. IGA is the alternative we explore here.

3 HIGAMod

The basic step of HiMOD consists of taking advantage of the particular shape of pipe domains by selecting different discretization procedures along axial and transverse directions. Any discretization technique can be in principle adopted.

In particular, the performance of the original HiMOD version may benefit from an approach able to achieve a higher accuracy with a low number of degrees of freedom. Moreover, since we aim at solving problems on potentially complex, curved domains (see Figure 3 below), it is desirable that the selected axial discretization scheme is based on functions characterized by high geometrical efficiency and flexibility. IGA is the ideal candidate.

We give hereafter a brief introduction to IGA and we present its fundamental ingredients. The Hierarchical IsoGeometric Approach for Model reduction (HIGAMod) follows straightforwardly from the standard HiMOD scheme replacing the finite element discretization along the axial fiber with an isogeometric one.

3.1 A brief introduction to Isogeometric Analysis

Isogeometric analysis was introduced by [21] in 2005 with the main aim of bridging the gap between Computer Aided Design (CAD) and Finite Element Analysis (FEA). The IGA paradigm is based on the adoption of the basis functions used for geometry representations in CAD systems - such as, e.g., B-Splines or Non-Uniform Rational B-Splines (NURBS) - also for the approximation of field variables, in an isoparametric fashion. This allows high geometric efficiency, accuracy, and flexibility, to go along with a cost-saving simplification of the typically expensive mesh generation and refinement processes required by standard FEA. Moreover, thanks to the high-regularity properties of its basis functions, IGA has shown better accuracy per-degree-of-freedom and enhanced robustness with respect to standard FEA in a number of applications ranging from solids and structures [11, 12, 15, 22, 24, 26] to fluids [1, 6, 25, 36] and fluid-structure interaction problems [7, 8, 20], opening also the door to geometrically flexible discretizations of higher-order partial differential equations in primal form [18, 23].

An IGA formulation basically relies on the use of spline shape functions within the main structure of a standard isoparametric finite element code; implementation details can be found in [13, 14]. As stated above, we aim at using IGA for the discretization of the HiMOD problem along the axial fiber, as an improvement relatively simple to implement but immediately leading to significant advantages in terms of reduced number of degrees of freedom and geometrical flexibility. Accordingly, in this manuscript we limit our description of IGA to the simple univariate, Galerkin case, and leave other possible extensions as future developments, as discussed in the final section.

3.1.1 Univariate B-Splines and NURBS

B-Splines are smooth approximating functions constructed by piecewise polynomials, and are the basic ingredient of most CAD systems. A B-Spline curve in $\mathbb{R}^d$ is obtained as the linear combination of B-Spline basis functions and some

coefficients ($\mathbf{B}_i$). These coefficients are points in $\mathbb{R}^d$, referred to as *control points*. For the sake of generality, in the remainder of this section we consider curves in $\mathbb{R}^3$ ($d = 3$), even if in our numerical tests we only consider plane problems ($d = 2$).

To define B-Spline functions we introduce a knot vector, i.e., a set of non-decreasing real numbers representing coordinates in the parametric space of the curve

$$\{\xi_1 = 0, ..., \xi_{n+p+1} = 1\}, \tag{5}$$

where p is the order of the B-Spline curve and n is the number of basis functions (and control points) necessary to describe it. The interval $[\xi_1, \xi_{n+p+1}]$ is called a patch. A knot vector is said to be uniform if its knots are uniformly-spaced and non-uniform otherwise. Moreover it is said to be open if its first and last knots have multiplicity $p + 1$. In what follows, we always employ open knot vectors. Basis functions formed from open knot vectors are interpolatory at the ends of the parametric interval $[0, 1]$ and are not, in general, interpolatory at interior knots.

Given a knot vector, univariate B-Spline basis functions are defined recursively as follows. For $p = 0$ (piecewise constants),

$$N_{i,0}(\xi) = \begin{cases} 1 \text{ if } \xi_i \leq \xi < \xi_{i+1} \\ 0 \text{ otherwise,} \end{cases} \tag{6}$$

for $p \geq 1$:

$$N_{i,p}(\xi) = \begin{cases} \dfrac{\xi - \xi_i}{\xi_{i+p} - \xi_i} N_{i,p-1}(\xi) + \dfrac{\xi_{i+p+1} - \xi}{\xi_{i+p+1} - \xi_{i+1}} N_{i+1,p-1}(\xi) \\ \qquad\qquad \text{if } \xi_i \leq \xi < \xi_{i+p+1}, \\ 0 \qquad\quad \text{otherwise,} \end{cases} \tag{7}$$

where, in (7), we set $0/0 = 0$. In Figure 1, we present the set of $n = 11$ B-Spline cubic basis functions generated from a particular open knot vector (specified in the caption).

If internal knots are not repeated, B-Spline basis functions are C^{p-1}-continuous. If a knot has multiplicity m the basis is C^k-continuous at that knot, where $k = p - m$. In particular, when a knot has multiplicity p, the basis is C^0 and interpolates the control point at that location (cf. Figure 1). Finally, B-Spline basis functions form a partition of unity, i.e., $\sum_{i=1}^{n} N_{i,p}(\xi) = 1$.

The generic B-Spline curve $\mathbf{S}$ is then defined by

$$\mathbf{S}(\xi) = \sum_{i=1}^{n} N_{i,p}(\xi)\mathbf{B}_i. \tag{8}$$

NURBS are defined starting from B-Splines with the additional property of representing exactly also conic sections. In $\mathbb{R}^3$, a NURBS curve is obtained starting from a set of "projective" control points denoted by $\mathbf{B}_i^w \in \mathbb{R}^4$ ($i = 1, ..., n$)

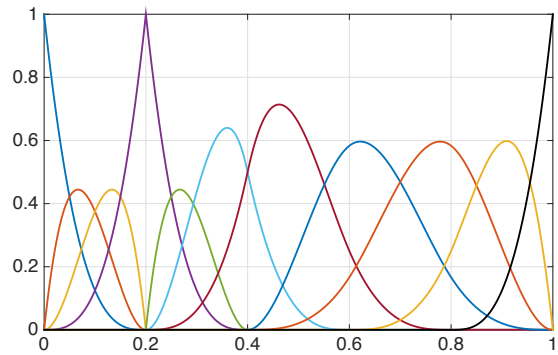

Figure 1: Cubic basis functions generated from the open knot vector $\{0, 0, 0, 0, 1/5, 1/5, 1/5, 2/5, 2/5, 3/5, 4/5, 1, 1, 1, 1\}$.

for a B-Spline curve in $\mathbb{R}^4$, and the corresponding shape functions $N_{i,p}(\xi)$. Then the control points for the NURBS curve in $\mathbb{R}^3$ are obtained by the following projection operation

$$[\mathbf{B}_i]_k = \frac{[\mathbf{B}_i^w]_k}{w_i}\ ,\ k = 1, 2, 3, \tag{9}$$

where $[\mathbf{B}_i]_k$ is the kth component of the vector $\mathbf{B}_i$ and $w_i = [\mathbf{B}_i^w]_4$ is referred to as the ith weight. The NURBS basis functions of order p are then defined as

$$R_{i,p}(\xi) = \frac{N_{i,p}(\xi) w_i}{\sum_{j=1}^{n} N_{j,p}(\xi) w_j}. \tag{10}$$

Due to the B-Spline partition of unity property, NURBS basis functions simply collapse to B-Spline basis functions if the weights are constant.

Analogously to the case of B-Splines, the corresponding NURBS curve $\mathbf{C}$ is finally obtained as

$$\mathbf{C}(\xi) = \sum_{i=1}^{n} R_{i,p}(\xi) \mathbf{B}_i. \tag{11}$$

As an example, in Figure 2, we present the quartic NURBS model of an helicoidal curve in $\mathbb{R}^3$, along with its control polygon (i.e., the piecewise linear interpolation of its control points).

We denote the support of the curve $\mathbf{C}$ by $\Gamma(\mathbf{C})$, hence $\Gamma(\mathbf{C}) \subset \mathbb{R}^3$. In addition, we suppose that the map $\mathbf{C} : [0, 1] \to \Gamma(\mathbf{C})$ is smooth and invertible, with smooth inverse denoted by $\mathbf{C}^{-1} : \Gamma(\mathbf{C}) \to [0, 1]$.

Following the isoparametric approach, the space of NURBS functions on $\Gamma(\mathbf{C})$ is defined as the span of the push-forward of the basis functions of (10), i.e., as

$$\mathcal{V}_n = \text{span}\{R_{i,p} \circ \mathbf{C}^{-1}, i = 1, \ldots, n\}. \tag{12}$$

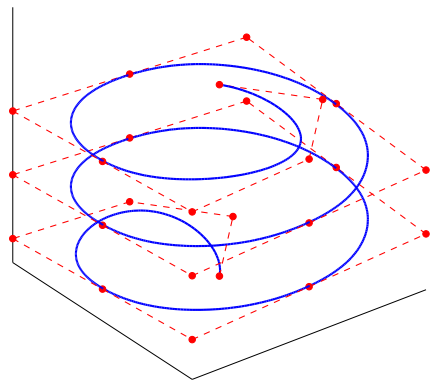

Figure 2: Quartic NURBS helicoidal curve, along with its control polygon (dotted).

Finally, note that the images of the knots through the function $\mathbf{C}$ naturally define a partition of the curve support $\Gamma(\mathbf{C}) \subset \mathbb{R}^3$. This partition identifies the mesh $\mathcal{M}_h$ associated with the discretization and is characterized by the mesh-size h. The latter is defined as the largest size of the elements in the mesh.

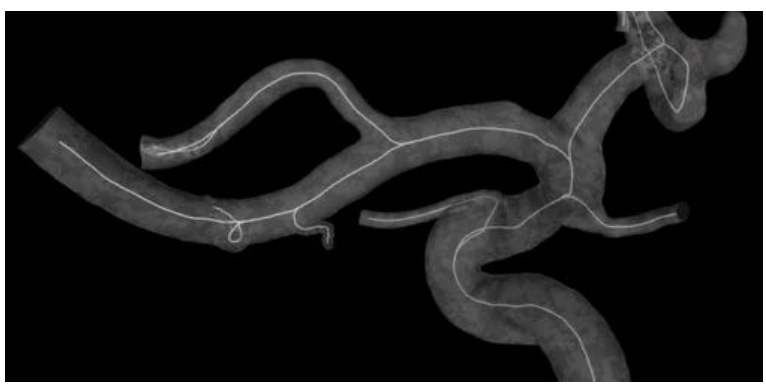

Figure 3: Reconstruction of a portion of a patient-specific cerebral vasculature. The centerline is highlighted. Image taken from the Aneuriskweb site [34].

3.2 HIGAMod in action

In practical applications of computational hemodynamics (as well in other fields of computational engineering) the domain of interest is often represented by a curved pipe with a nontrivial centerline. For the sake of exemplification, in Fig-

ure 3 we illustrate the reconstruction of a portion of cerebral vessels obtained by rotational angiographies and performed by the open source code Vascular Modeling ToolKit (VMTK) [4] within the Aneurisk Project. The data are available at the AneuriskWeb site [34]. VMTK performs first a pointwise description of the centerline and successively a spline approximation [33]. Alternative approximations are possible [35].

Referring to the picture, the white centerline can be split into segments $\Gamma_k(\mathbf{C})$ connected at the bifurcations. Each $\Gamma_k(\mathbf{C})$ represents the domain Ω_{1D} that we equip with the NURBS functional representation (11). The map $\mathbf{C}$ coincides therefore with the HiMod map Ψ for each segment and the reference 1D domain $\widehat{\Omega}_{1D}$ is locally given by the interval $[0, 1]$. The HIGAMod formulation of a linear advection diffusion reaction problem is therefore promptly retrieved from (4) where we replace the 1D functions $\vartheta(\widehat{x})$ with the NURBS (10).

In practice, assembly and solution of the problem can proceed as for the original finite-element based HiMod discretization, with the only attention to be paid to the judicious selection of the degree of exactness of the Gauss-Legendre quadrature formulas to guarantee an appropriate control of the integration error.

4 Numerical results

We illustrate preliminary results obtained for HIGAMod applied to both linear ADR problems (3) as well as to the classical Stokes problem in the classical velocity-pressure formulation

$$\begin{cases} -\mu\Delta\mathbf{u} + \nabla P = 0 \\ \nabla\cdot\mathbf{u} = 0 \end{cases} \quad \text{in } \Omega \tag{13}$$

where $\mathbf{u}$ denotes the velocity and P the pressure of an incompressible fluid. We consider both rectilinear and curved pipes. When an analytical solution is available, we also assess the beneficial effect of the continuity, comparing in particular maximum continuity IGA results with those obtained when the continuity is reduced to C^0 (when considering isoparametric p-FEA).

We finally highlight that in all the results we present we use Legendre polynomials to model the transverse components, even if it is clearly possible to choose different modal basis, such as, e.g., sinusoidal functions.

We will use the classical abridged notation L^2 and H^1 to denote the Sobolev spaces $L^2(\Omega)$ and $H^1(\Omega)$ respectively.

4.1 Test 1: ADR problems

Referring to equation (3) for several possible domains Ω, we compare the L^2- and the H^1-norm of the approximation errors of HIGAMod using C^1 quadratic basis functions with the results of HiMod (using C^0 quadratic basis functions

instead of classical linear finite elements). Transverse components are modeled with $m = 3$ Legendre polynomial modes.

More specifically, the second and the third cases refer to curvilinear domains, where (s, t) denote the curvilinear and the transverse coordinates of the centerline, respectively.

All the cases are solved with homogeneous Dirichlet conditions on the sides of the pipe as well as at the inflow boundary, while a homogeneous Neumann condition holds at the outflow. More general boundary conditions can be considered as well, following the guidelines of [3]. The ADR parameters are assumed to be $\mu = 1$, $\mathbf{b} = [1; 0]$ and $\sigma = 0$.

4.1.1 Rectangular domain

In this first case, the domain is $\Omega = (0, 1) \times (-0.5, 0.5)$. The forcing term is set such that the solution is $u_{ex}(x, y) = (-0.2x^5 - 0.5x^2)\sin[2\pi(y + 0.5)]$.

L^2- and H^1-norm of the relative errors are reported in Figure 4. It is possible to observe that the expected optimal convergence rates are attained by both quadratic HIGAMod and HiMOD formulations; however a superior accuracy is obtained on a per-degree-of-freedom basis thanks to the higher continuity guaranteed by HIGAMod.

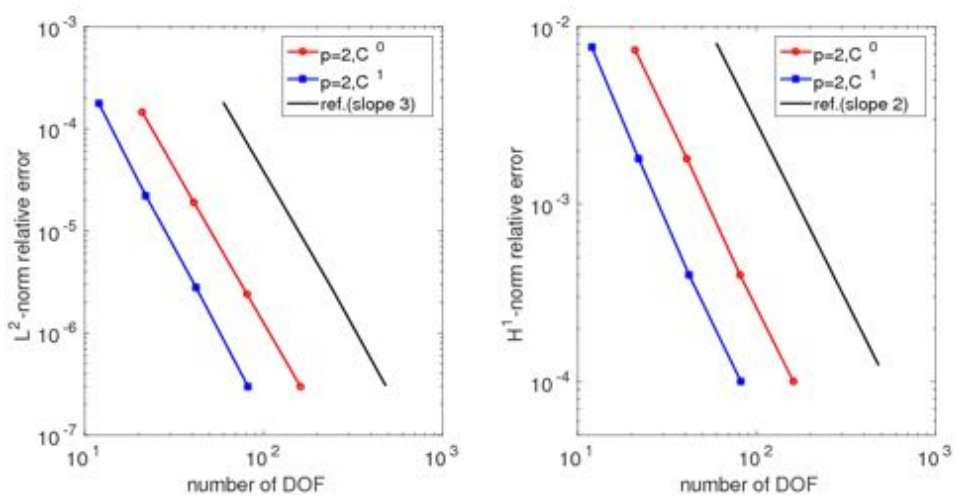

Figure 4: ADR on a rectangular domain. Relative L^2-norm (left) and H^1-norm (right) errors for HIGAMod (blu) and HiMOD (red). The black solid line indicates the optimal convergence rates.

4.1.2 Curvilinear domains

We considered two cases where we still solve the ADR problem (3) in curvilinear domains. We consider the cases of a centerline described by both a parabolic and a cubic polynomial. The analytical solutions are assumed to be $u_{ex}(s,t) = (0.25s^4 - L^3 s)\sin[2\pi(t+0.5)]$, with $L = \int_0^1 \sqrt{1+4x^2}dx$, for the parabolic case and $u_{ex}(s,t) = (0.2s^5 - L^4 s)\sin[2\pi(t+0.5)]$, with $L = \int_0^1 \sqrt{1+9x^4}dx$, for the cubic case. The corresponding forcing terms have been built accordingly. For the sake of brevity, we report here only the case of cubic centerline, since we found similar results of the parabolic case - see Fig. 5.

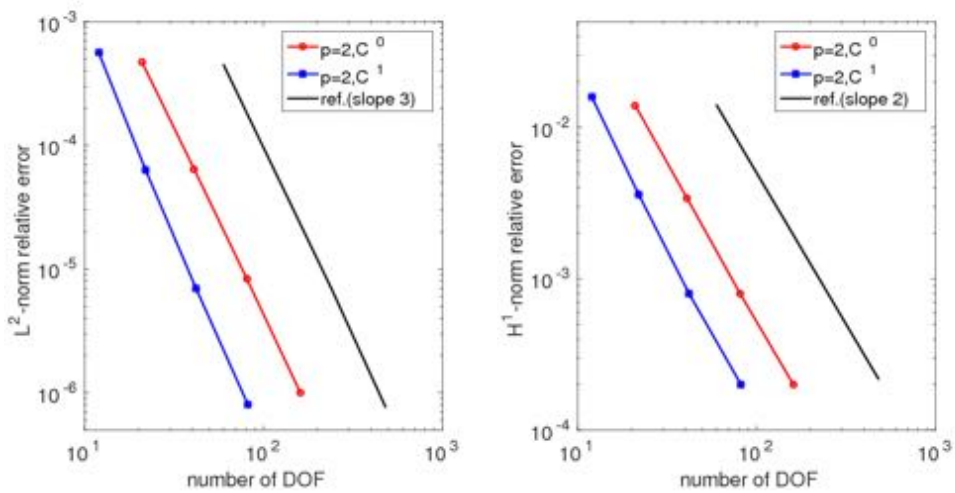

Figure 5: ADR on a curvilinear domain with a cubic centerline. Relative L^2-norm (left) and H^1-norm (right) errors for HIGAMod (blue) and HiMOD (red). The black solid line indicates the optimal convergence rates.

Similarly to the rectangular case, the approximations exhibit the expected convergence orders, however HIGAMod outperforms the original HiMod for the reduction of degrees of freedom when the accuracy is comparable. This prospects a sensible advantage of the computational costs for 3D nontrivial problems.

4.2 Stokes results

Let us consider the Stokes problem (13). Again, we focus on three test cases, characterized by different shapes of the domain. The first two tests have been designed such that an analytical solution is available, while for the third one we use as a reference the full 2D finite element solution obtained with a $\mathbb{P}^2\mathbb{P}^1$ mixed formulation. In all tests, we assume $\mu = 1$.

4.2.1 Rectangular domain

The first case is defined on $\Omega = (0, 10) \times (-1, 1)$. On the inflow boundary a Dirichlet condition imposes the classical parabolic profile of u_x, while on the upper and the lower parts of the boundary, homogeneous Dirichlet conditions are imposed on both components of the velocity field. Finally, a homogeneous Neumann condition si imposed at the outflow. The volumic forcing term is assumed to have components $f_x(x, y) = 2 - \pi/2 \sin(\pi x/20)$ and $f_y(x, y) = 0$. The solution corresponding to the described setting is reported in Figure 6.

Along the axial direction, we consider a mixed velocity-pressure formulation with quadratic ($p = 2$) and cubic ($p = 3$) approximation for the pressure, with continuity varying between C^0 and C^{p-1}, and an approximation one degree higher (but with the same continuity) for the velocity. The transverse components are modeled with $m = 5$ Legendre polynomial modes. In Figure 7 we show the obtained convergence plots in terms of relative L^2-norm error for the pressure (we do not show the analogue plots for the velocity since for this problem it is exactly represented by our approximation space). From the plots, it is possible to clearly observe the beneficial effect of continuity. As a matter of fact, the same considerations done for the ADR case are valid also for the steady Stokes problem. Notice that, for the setting adopted to solve this problem, the accuracy limit for the relative L^2-norm error for the pressure results to be in the order of 10^{-7}.

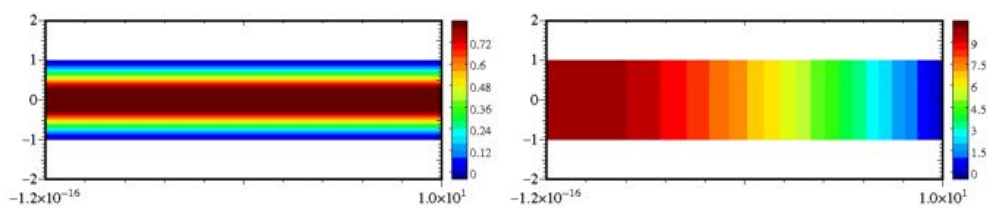

Figure 6: Stokes on a rectangular domain. Contour plots of the analytical solution for the velocity magnitude (left) and the pressure (right).

4.2.2 Curvilinear domain

The second case is obtained from the previous one mapping the load, the boundary conditions, and, as a consequence, the solution to reproduce the same problem on a curvilinear domain characterized by a quartic profile of the centerline. The solution corresponding to the described setting is reported in Figure 8.

Also here, along the axial direction, we consider a mixed velocity-pressure formulation with quadratic ($p = 2$) and cubic ($p = 3$) approximation for the pressure. Consequently continuity ranges between C^0 and C^{p-1} for the pressure

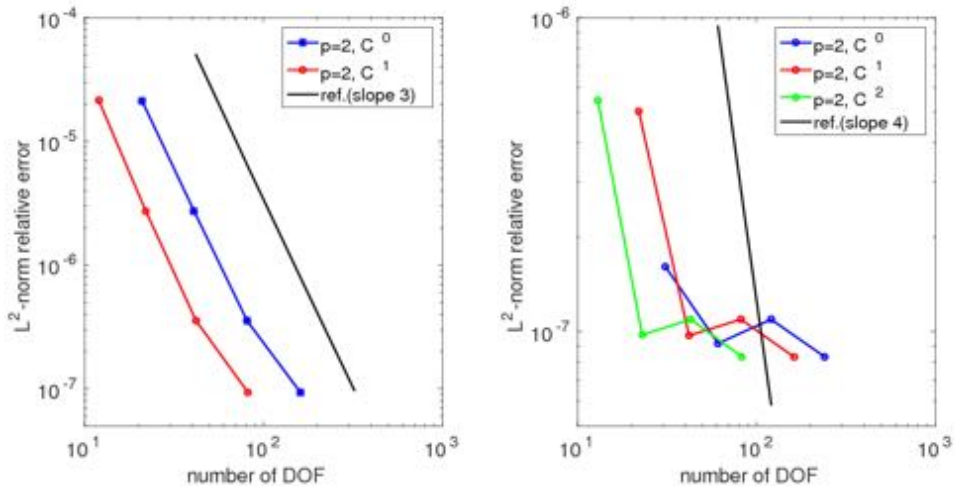

Figure 7: Stokes on a rectangular domain. Relative L^2-norm for the pressure using quadratic (left) and cubic (right) approximations for different continuity choices.

and C^1 and C^p for the velocity. The transverse components are modeled with $m = 5$ Legendre polynomial modes. In Figure 9 we show the obtained convergence plots in terms of relative L^2-norm error for the pressure (we do not show the analogue plots for the velocity since for this problem it is exactly represented by our approximation space). From the plots it is possible to clearly observe the beneficial effect of continuity also in a curvilinear case, and considerations very similar to those regarding the previous case can be stated here.

4.3 Complex curvilinear domain

We conclude our numerical campaign with a steady Stokes problem characterized by a complex geometry with a sinusoidal profile and a decreasing thickness. Homogeneous Dirichlet conditions are imposed on both upper and lower sides of the domain, while on both inflow and outflow sides homogeneous Neumann conditions are applied. Finally, a pressure drop $\Delta p = 5$ is imposed (as it typically happens in many fluid-dynamics applications).

The problem has been solved using the same HIGAMod formulation adopted in the previous tests (quadratic pressure and cubic velocity, with C^1 continuity for both fields), considering an increasing DOF number in the axial direction and an increasing number of transverse modes. Convergence is obtained as expected and the finest obtained solution (corresponding to 1,002 velocity DOF, 502 pressure DOF, and 17 transverse modes) is reported on the left of Figures 10 and 11. Since an analytical solution is not available, a reference solution has

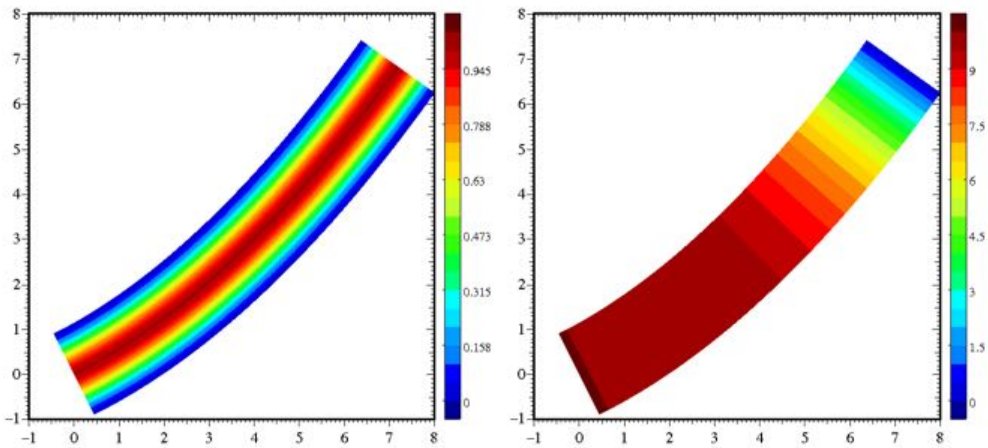

Figure 8: Stokes on a curvilinear domain with a quartic centerline. Contour plots of the analytical solution for the displacement magnitude (left) and the pressure (right).

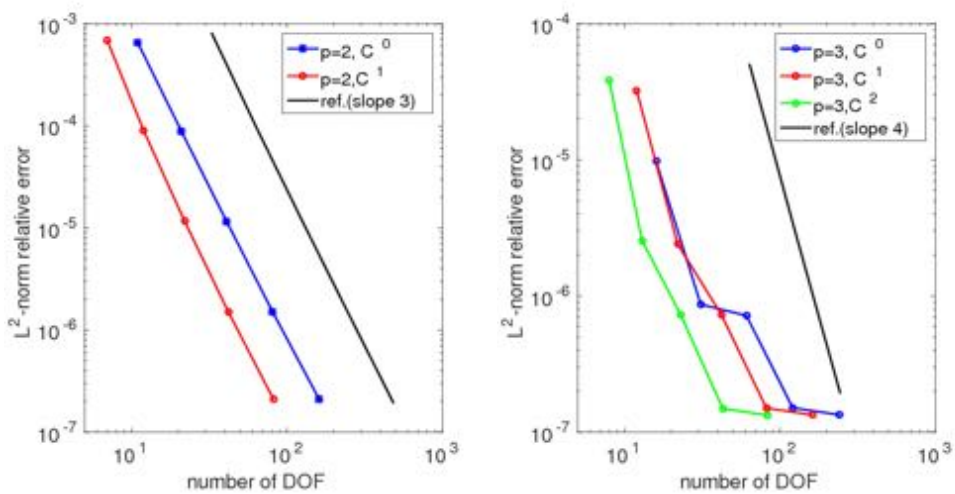

Figure 9: Stokes on a curvilinear domain with a quartic centerline. Relative L^2-norm for the pressure using quadratic (left) and cubic (right) approximations for different continuity choices.

been computed using the $\mathbb{P}^2\mathbb{P}^1$ mixed FEM formulation available in the software `FreeFem++`[19]. Such a solution is reported on the right of Figures 10 and 11 and has been obtained using a mesh of 165,803 triangles, corresponding to 334,846 velocity DOF and 84,522 pressure DOF. In spite of the difference of the size of the discretized problems, an excellent agreement between the proposed HIGAMod and full FEM results is promptly observed. This confirms the HIGAMod capability of accurately reproducing even very complex solutions, at a fraction of the cost.

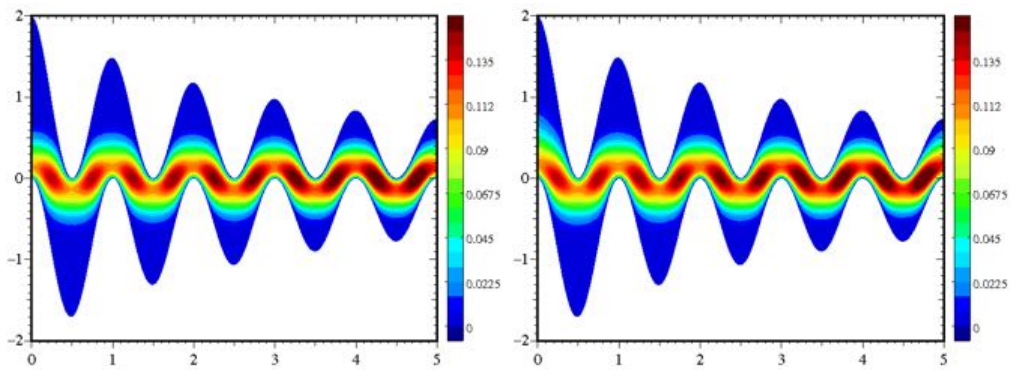

Figure 10: Stokes on a curvilinear domain with a sinusoidal profile and a decreasing thickness. Contour plots of the numerical solution for the displacement magnitude obtained with HIGAMod (left) and full finite elements (right).

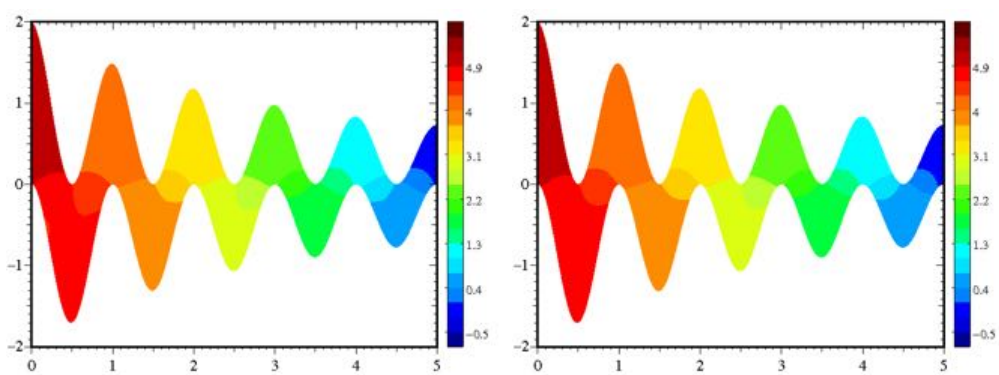

Figure 11: Stokes on a curvilinear domain with a sinusoidal profile and a decreasing thickness. Contour plots of the numerical solution for the pressure obtained with HIGAMod (left) and full finite elements (right).

5 Conclusions

Stimulated by emerging applications of computational fluid dynamics, in particular for coronary and aortic diseases, we need to improve simplified 1D network models as well as to reduce computational costs of 3D solutions [17]. The HiMod reduction was intended to address this problem, by enhancing a 1D finite element solution and reducing the number of degrees of freedom of a 3D solver. The approach suffers from some limitations in treating curved pipes that can be removed by switching to isogeometric approximations for the axial components. This paper proposes the first steps in this direction, which are corroborated by very promising preliminary results.

As this opens new perspectives for the set up of efficient solvers in computational hemodynamics, several questions need to be answered and will be the subject of forthcoming papers. At the theoretical level, we need to address the inf-sup condition for the approximation of the Stokes problem and in particular to analyze the combination of discrete schemes for velocity and pressure that guarantee the non singularity of the discretization. In addition, we need to explore possible evolution of the scheme such as the combination of diverse IGA approximations within the directional splitting of HiMod for both axial and transverse dynamics. Another research direction to be explored consists of the use of efficient IGA collocation schemes (see, e.g., [5]) for the discretization along the centerline. Finally, the results presented here need to be extended to the 3D settings for academic as well as real patient-specific test cases, toward a strong integration between image processing tools and numerical solvers.

Acknowledgments

A. Veneziani and S. Perotto acknowledge the support of the National Science Foundation - Project DMS 1419060 “Hierarchical Model Reduction Techniques for Incompressible Fluid Dynamics and Fluid-Structure Interaction Problems” (2014-2017). A. Reali acknowledges the support of the European Research Council through the FP7 Ideas Starting Grant “ISOBIO: Isogeometric Methods for Biomechanics” (project # 259229).

References

References

[1] Akkerman, I., Bazilevs, Y., Calo, V.M., Hughes, T.J.R., Hulshoff, S. The role of continuity in residual-based variational multiscale modeling of turbulence. Comput. Mech. **41**, 371–378 (2008)

[2] Aletti, M., Bortolossi, A., Perotto, S., Veneziani, A. One-dimensional surrogate models for advection-diffusion problems. In: Abdulle, A., Deparis,

S., Kressner, D., Nobile, F., Picasso, M. (eds.), Numerical Mathematics and Advanced Applications, Lect. Notes Comput. Sci. Eng., Vol. **103**, pp. 447–456. Springer (2015)

[3] Aletti, M., Perotto, S., Veneziani, A. Educated bases for the HiMod reduction of advection-diffusion-reaction problems with general boundary conditions. MOX Report no. **37/2015** (2015)

[4] Antiga, L., Piccinelli, M., Botti, L., Ene-Iordache, B., Remuzzi, A., Steinman, D. A. An image-based modeling framework for patient-specific computational hemodynamics. Med. Biol. Eng. Comput. **46**(11), 1097–1112 (2008)

[5] Auricchio, F., Beirão da Veiga, L., Hughes, T.J.R., Reali, A., Sangalli, G. Isogeometric Collocation Methods. Math. Mod. Meth. Appl. Sci., **20**, 2075–2107 (2010)

[6] Bazilevs, Y., Calo, V.M., Cottrell., J.A., Hughes, T.J.R., Reali, A., Scovazzi, G. Variational multiscale residual-based turbulence modeling for large eddy simulation of incompressible flows. Comput. Methods Appl. Mech. Engrg. **197**, 173–201 (2007)

[7] Bazilevs, Y., Calo, V.M., Hughes, T.J.R., Zhang, Y. Isogeometric fluid-structure interaction: Theory, algorithms, and computations. Comput. Mech. 43, 3–37 (2008)

[8] Bazilevs, Y., Hsu, M.-C., Kiendl, J., Wuchner, R., Bletzinger, K.U. 3D simulation of wind turbine rotors at full scale. part II: Fluid-structure interaction modeling with composite blades. Int. J. Numer. Meth. Fluids **65**, 236–253 (2011)

[9] Blanco, P.J., Leiva, J.S., Feijóo, R.A., Buscaglia, G.C. Black-box decomposition approach for computational hemodynamics: one-dimensional models. Comput. Methods Appl. Mech. Engrg. **200**(13-16), 1389–1405 (2011)

[10] Blanco, P. J., Alvarez, L. M., Feijóo, R. A. Hybrid element-based approximation for the Navier-Stokes equations in pipe-like domains. Comput. Methods Appl. Mech. Engrg. **283**, 971–993 (2015)

[11] Borden, M., Verhoosel, C., Scott, M., Hughes, T.J.R., Landis, C. A phase-field description of dynamic brittle fracture. Comput. Methods Appl. Mech. Engrg. **217-220**, 77–95 (2012)

[12] Caseiro, J., Valente, R., Reali, A., Kiendl, J., Auricchio, F., Alves de Sousa, R. Assumed natural strain NURBS-based solid-shell element for the analysis of large deformation elasto-plastic thin-shell structures. Comput. Methods Appl. Mech. Engrg. **284**, 861–880 (2015)

[13] Cottrell, J.A., Hughes, T.J.R., Bazilevs, Y. Isogeometric Analysis Toward Integration of CAD and FEA, Wiley, 2009.

[14] de Falco, C., Reali, A., Vazquez, R. GeoPDEs: a research tool for IsoGeometric Analysis of PDEs. Adv. Eng. Softw. **42**, 1020–1034 (2011)

[15] Elguedj, T., Bazilevs, Y., Calo, V.M., Hughes, T.J.R. $\overline{B}$ and $\overline{F}$ projection methods for nearly incompressible linear and non-linear elasticity and plasticity using higher-order NURBS elements. Comput. Methods Appl. Mech. Engrg. **197**, 2732–2762 (2008)

[16] Ern, A., Perotto, S., Veneziani, A. Hierarchical model reduction for advection-diffusion-reaction problems. In: Kunisch, K., Of, G., Steinbach, O. (eds.), Numerical Mathematics and Advanced Applications, pp. 703–710. Springer-Verlag (2008)

[17] Peiró, J., Veneziani A. Reduced models of the cardiovascular system. In: Formaggia, L., Quarteroni, A., Veneziani, A. (eds.), Cardiovascular Mathematics, Modeling, Simulation and Applications, Vol. **1**, pp. 347–394, Springer-Verlag, Berlin, Heidelberg (2009)

[18] Gomez, H., Calo, V.M., Bazilevs, Y., Hughes, T.J.R. Isogeometric analysis of the Cahn-Hilliard phase-field model, Comput. Methods Appl. Mech. Engrg. **197**, 4333–4352 (2008)

[19] Hecht., F. New developement in FreeFem++. J. Numer. Math. **20**(3-4), 251–265 (2012)

[20] Hsu, M.-C., Kamensky, D., Xu, F., Kiendl, J., Wang, C., Wu, M.C.H., Mineroff, J., Reali, A., Bazilevs, Y., Sacks, M.S. Dynamic and fluid-structure interaction simulations of bioprosthetic heart valves using parametric design with T- splines and Fung-type material models. Comput. Mech. **55**, 1211–1225 (2015)

[21] Hughes, T.J.R., Cottrell, J.A., Bazilevs, Y. Isogeometric analysis CAD, finite elements, NURBS, exact geometry and mesh refinement. Comput. Methods Appl. Mech. Engrg. **194**, 4135–4195 (2005)

[22] Hughes, T.J.R., Evans, J.A., Reali, A. Finite element and NURBS approximations of eigenvalue, boundary-value, and initial-value problems. Comput. Methods Appl. Mech. Engrg. **272**, 290–320 (2014)

[23] Kiendl, J., Hsu, M.-C., Wu, M.C.H., Reali, A. Isogeometric Kirchhoff-Love shell formulations for general hyperelastic materials. Comput. Methods Appl. Mech. Engrg. **291**, 280–303 (2015)

[24] Lipton, S., Evans, J.A., Bazilevs, Y., Elguedj, T., Hughes, T.J.R. Robustness of isogeometric structural discretizations under severe mesh distortion. Comput. Methods Appl. Mech. Engrg. **199**, 357–373 (2010)

[25] Liu, J., Gomez, H., Evans, J.A., Hughes, T.J.R., Landis, C.M. Functional entropy variables: A new methodology for deriving thermodynamically consistent algorithms for complex fluids, with particular reference to the isothermal Navier–Stokes–Korteweg equations. J. Comput. Phys. **248**, 47–86 (2013).

[26] Morganti, S., Auricchio, F., Benson, D.J., Gambarin, F.I., Hartmann, S., Hughes, T.J.R., Reali, A. Patient-specific isogeometric structural analysis of aortic valve closure. Comput. Methods Appl. Mech. Engrg. **294**, 428–448 (2015)

[27] Perotto, S. A survey of hierarchical model (Hi-Mod) reduction methods for elliptic problems. In: Idelsohn, S.R. (ed), Numerical Simulations of Coupled Problems in Engineering, Computational Methods in Applied Sciences, Vol. **33**, pp. 217–241, Springer (2014)

[28] Perotto, S. Hierarchical model (Hi-Mod) reduction in non-rectilinear domains. In: Erhel, J., Gander, M., Halpern, L., Pichot, G., Sassi, T., Widlund, O. (eds.), Domain Decomposition Methods in Science and Engineering, Lect. Notes Comput. Sci. Eng., Vol. **98**, pp. 477–485, Springer, Cham (2014)

[29] Perotto, S., Ern, A., Veneziani, A. Hierarchical local model reduction for elliptic problems: a domain decomposition approach. Multiscale Model. Simul. **8**(4), 1102–1127 (2010)

[30] Perotto, S., Veneziani, A. Coupled model and grid adaptivity in hierarchical reduction of elliptic problems. J. Sci. Comput. **60**(3), 505–536 (2014)

[31] Perotto, S., Zilio, A. Hierarchical model reduction: three different approaches. In: A. Cangiani, R. Davidchack, E. Georgoulis, A. Gorban, J. Levesley, M. Tretyakov (eds.), Numerical Mathematics and Advanced Applications, pp. 851-859, Springer-Verlag (2013)

[32] Perotto, S., Zilio, A. Space-time adaptive hierarchical model reduction for parabolic equations. Adv. Model. and Simul. in Eng. Sci. **2**: 25 (2015).

[33] Piccinelli, M., Veneziani, A., Steinman, D., Remuzzi, A., Antiga, L. A framework for geometric analysis of vascular structures: application to cerebral aneurysms. IEEE T. Med. Imaging, **28**(8), 1141–1155 (2009)

[34] http://mathcs.emory.edu/aneuriskweb

[35] Sangalli, L. M., Secchi, P., Vantini, S., Veneziani, A. Efficient estimation of three-dimensional curves and their derivatives by free-knot regression splines, applied to the analysis of inner carotid artery centrelines. J. Roy. Stat. Soc. C-App., **58**(3), 285–306 (2009)

[36] Zhang, Y., Bazilevs, Y., Goswami, S., Bajaj, C., Hughes, T.J.R. Patient-specific vascular NURBS modeling for isogeometric analysis of blood flow. Comput. Methods Appl. Mech. Engrg. **196**, 2943–2959 (2007)